International Journal of Microwave and Wireless Technologies, 2013, 5(5), 637–644.
doi:10.1017/S1759078713000548

RESEARCH PAPER

Linear array modules with prescribed excitations using waveguide shunt slot-fed microstrip patch elements

KHAGINDRA SOOD[1], RAJEEV JYOTI[1] AND SHASHI BHUSHAN SHARMA[2]

A waveguide shunt slot-fed microstrip patch antenna (WGMPA) element is proposed and analyzed with method of moments (MOM) using entire-domain basis functions. The developed analysis has been utilized to obtain parametric observation of power-coupling versus transverse offset of feeding slot from the waveguide axis. Expressions for the radiation pattern as a summation of contributions of individual basis functions are reported. The proposed element is amenable to building-up series-fed linear arrays by a simple cascading of elements at the through-end of the feeding waveguide. The authors propose that arbitrary amplitude excitations may be applied to such linear arrays for desired tailored array pattern characteristics. The required transverse offsets for each array element may be computed using the reported parametric result. As a demonstration of concept, two distributions are designed – uniform amplitudes and Dolph–Chebyshev for reduced side lobes. Computed element patterns from MOM are used with an array factor formulation for arbitrary element positions. Both modules show radiation characteristics closely matching the expected directivity and sidelobe envelopes. Analysis validation is achieved using a proven finite element method (FEM)-based solver; the comparison is close and is reported. Efficacy of the waveguide shunt-slot fed patch element for building linear array modules with prescribed amplitude distributions is thus established.

Keywords: Antennas and propagation for wireless system, Antenna design, Modeling and measurements

Received 6 November 2012; Revised 25 April 2013; first published online 3 June 2013

I. INTRODUCTION

Aperture-coupled feeds for a microstrip patch antenna were first proposed by Pozar [1]. Excitation typically occurs electromagnetically through a ground-plane aperture from a feed line on one side to the radiator on its other side. Kanda *et al.* have proposed a waveguide aperture-coupled feed through an end-wall slot [2] that has been studied further by Ho and Hsu [3]. In the present paper, a waveguide top-wall slot is suggested instead as a mechanism of patch excitation. As compared to the end-wall slot, in this radiator configuration, antenna elements may be conveniently cascaded to obtain a series-fed linear array. The term "*stick*" array has been used to denote this kind of linear array configuration. Chang and Schaubert have investigated such arrays using inclined side-wall slots to excite the patch elements [4]. Furthermore, this may be employed as a sub-array by repeating units across the waveguide axis to obtain a planar array. The patch being resonant, allows the slot itself to be relatively short and the inter-stick spacing may be maintained optimum for avoiding grating lobes [4]. An apparent disadvantage of this feed is that the slot inclination must be altered to change the excitation amplitude that leads to polarization issues. With the proposed shunt-slot scheme, slots may be retained collinear and only their offsets suffice to control the coupling amplitude.

With this inspiration, the proposed waveguide shunt slot-fed microstrip patch antenna (WGMPA) is analyzed using a method of moments (MOM) formulation to investigate the configuration and obtain design guidelines. Entire-domain basis functions in conjunction with a Galerkin procedure have been used to obtain an accurate numerical solution for problem geometry. The MOM analysis has been used to obtain variation of the coupled power from the longitudinal slot with transverse offset. The reciprocity method has been used to compute the far-field contributions of individual MOM-matrix coefficients. The actual element radiation pattern is thus obtained as a weighted summation of the pattern contributions term-by-term.

Coming to the design of the linear array itself, a centrally-positioned longitudinal slot is not expected to radiate; a pre-calculated transverse offset is necessary. Successive slots need not be spaced a guide-wavelength apart, as may appear at first glance. By alternately displacing slots to either side of the long axis of the waveguide, the slots can be positioned $\lambda_g/2$ apart and yet radiate in phase. For the desired amplitude excitations, the corresponding slot transverse offsets are obtained from the MOM analysis. This method of feeding a linear array may be applied for any chosen number of elements with an arbitrary amplitude distribution.

[1]Space Applications Centre (ISRO), Ahmedabad, India.
[2]Indus Institute of Engineering & Technology, Ahmedabad, India.
Corresponding author:
Khagindra Sood
Email: khagindras@yahoo.co.in

In this paper, the proposed shunt slot-fed patch element has been used to realize two types of linear array modules using alternating side-to-side slot placement. The modules consist of five elements each and are general cases of (i) uniformly-excited linear array and (ii) linear array with a tailored Dolph–Chebyshev distribution for reduced side lobes. For the latter case, the amplitude tapers are provided by varying the slot transverse offset along the length of the array. As the choice of tapers is completely general, the present study is expected to establish the suitability of the proposed element for realizing such linear array "*sticks*". Suitable precautions like central feeding are still necessary when planning an operational linear/planar array to ensure that frequency-scanning is avoided as shown in [5].

We present the design and analysis of these two linear array modules based on the MOM-analysis in conjunction with an array factor formulation for arbitrary element positions. The two sample linear array modules are also analyzed using an FEM-based commercial electromagnetic (e.m.) solver for the sake of validation. Prototype design is carried out at C-band and the results from the two analyses are compared.

Compared to the aperture-coupled microstrip line feed, fringing fields in the waveguide feed are completely enclosed in the rear half-space; minimizing spurious back-lobe radiation. Also, spurious coupling to (active) devices, if any, is reduced. Thus, the proposed feeding method would be suitable for active antenna array applications. Also, at higher microwave or mm-wave bands, the microstrip line losses become progressively prohibitive. Substrate thickness must be reduced to preclude surface wave generation resulting in a mechanically flimsy structure. Waveguide feeding lends a robust structure with very low feed line losses.

II. MOM-ANALYSIS OF THE WGMPA ELEMENT

WGMPA element geometry is illustrated in Fig. 1. The patch radiator on the microstrip substrate is centered above the waveguide top-wall slot. The original problem may be decoupled using the equivalence principle; closing the coupling slot with a perfect magnetic conductor. Anti-parallel magnetic currents are assumed across the slot in the respective "half"-problems. This is a sheet magnetic current density represented by $\bar{M}$V/m across the slot and is defined by the relation $\bar{M} = \bar{E} \times \hat{n}$, where $\bar{E}$ is the steady-state electric field across the slot and $\hat{n}$ is the unit outward normal across the plane of the slot. The two sub-problems may be separately solved with the magnetic current as a common coupling source. The other unknown is $\bar{J}$ A/m which is the sheet electric density across the patch surface.

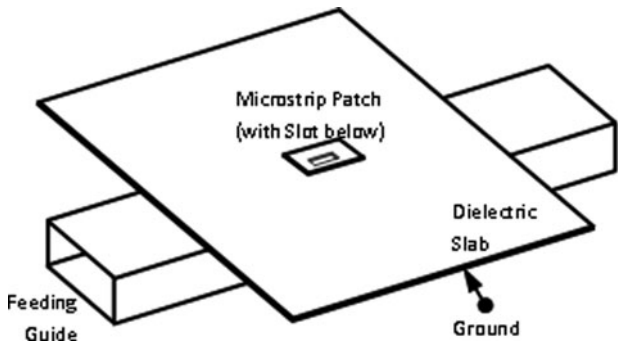

Fig. 1. WGMPA (single-element) geometry.

Following the MOM procedure, two operator equations representing the problem of Fig. 1 are obtained

$$\bar{H}_t^a(\bar{M}) + \bar{H}_t^b(\bar{M}) - H_t^b(\bar{J}) = \bar{H}_t^{inc} \text{across } S_1 \tag{1}$$

$$-\bar{E}_t^a(\bar{M}) + \bar{E}_t^b(\bar{J}) = 0 \text{ across } S_2, \tag{2}$$

where S_1 denotes the slot and S_2 the patch surface. The subscript, 't' denotes the tangential component; 'a' is the waveguide sub-problem and 'b' the upper half-space e.g. $\bar{E}_t^b(\bar{J})$ is the tangential electric field in region 'b' due to the patch electric current.

The unknown currents are expanded as in terms of a series of known current functions with unknown coefficients as:

$$\bar{M} = \sum_{m=1}^{N^a} V_m \bar{M}_m; \quad and \quad \bar{J} = \sum_{i=1}^{N^b} I_1 \bar{J}_i. \tag{3}$$

Following the MOM procedure, (1) and (2) may be converted to the MOM matrix equation that is:

$$\begin{pmatrix} [Y^a + Y^b] & [T^b] \\ [C^b] & [Z] \end{pmatrix} \begin{pmatrix} \bar{V}_m \\ \bar{I}_l \end{pmatrix} = \begin{pmatrix} \bar{I}_i \\ 0 \end{pmatrix}, \tag{4}$$

where Y^a, Y^b are self-admittance parameters for regions 'a' and 'b', respectively. T^b and C^b are the patch-to-slot coupling terms and vice versa, while Z is a self-impedance for the patch. V_m and I_l are column vectors denoting the unknown coefficients. I_i is the excitation vector due to the incident signal at waveguide port while excitation in the patch region is the null vector (excitation occurs through the two coupling terms). The moment matrix is of order $(N^a + N^b) \times (N^a + N^b)$, where N^a, N^b are the maximum number of functions retained for slot and patch respectively where the series in (3) are truncated. The matrix terms are obtained by taking the inner product of the relevant expansion function with the selected weighting function.

Although the formulation is general, we report the specific case of a rectangular slot exciting a rectangular patch radiator. Entire-domain sinusoidal functions are used as the basis functions as well as testing functions (in accordance with Galerkin's procedure). The solution, i.e., the values of the coefficient vector in (4) are obtained by inverting the MOM-matrix and pre-multiplying it to the R.H.S. The MOM- coefficients thus obtained can be used to compute the network parameters of the structure in Fig. 1 as well as its far-field.

Details of the MOM derivation, expressions for the matrix terms and network parameters, and parametric studies with regard to the chief design variables have been reported by the authors separately [6]. Only coupled power variation with slot transverse offset and expressions for the far-field quantities are included here as these are relevant for succeeding computations on linear arrays.

https://doi.org/10.1017/S1759078713000548 Published online by Cambridge University Press

III. PARAMETRIC VARIATION OF COUPLED POWER AND FAR-FIELD CONTRIBUTIONS

Parametric study for power coupling through slot versus transverse offset was carried out for a C-band prototype by a series of swept–frequency responses using the developed MOM-analysis. Coupled power is the balance from s_{11} and s_{21}.

The design variable set for the C-band prototype is:

Waveguide: WR-159 $a \times b = 40.39$ mm $\times$ 20.19 mm;
Substrate: Rogers RO-3003 $\varepsilon_r = 3.0$; tan $\delta = 0.0013$; Thickness, $d = 1.524$ mm
Microstrip patch: $L_p \times W_p = 14.12$ mm $\times$ 9.41 mm
and Coupling slot: $L_s \times W_s = 4.0$ mm $\times$ 0.5 mm
Patch position: $x_p = 0.0$ mm and $y_p = 0.0$ mm
Coupling slot offset: $x_p = 30.195$ mm (offset = 10.0 mm)

The slot offset from the waveguide axis varied from zero (centered, no-coupling position) to maximum permissible without cutting the end-wall. One observes zero-coupling at the start, a monotonic increase in coupling from about 2.0 to 12.0 mm beyond which the response appears to saturate (Fig. 2). This last region is not recommended as return loss fluctuates [6].

The radiation pattern of the WGMPA element is a vector sum of the far-field contributions of individual basis functions, i.e. patch electric current (dominant) and slot magnetic current (minor). An elementary dipole is assumed at the far-field point. From an *a priori* knowledge of its field at the WGMPA position, the reciprocity theorem allows the desired far-field to be computed. The complete expression in matrix notation is:

$$E_m = -\frac{jK_0\eta}{4\pi r_m} e^{-jk_0 r_m} [\,\bar{P}^{m1} \quad \bar{P}^{m2}\,] \begin{pmatrix} \bar{I} \\ \bar{V} \end{pmatrix}, \tag{5}$$

where $\bar{P}^{m1}$, $\bar{P}^{m2}$ are termed measurement vectors. The evaluated coefficients substituted in (5) give the net far-field.

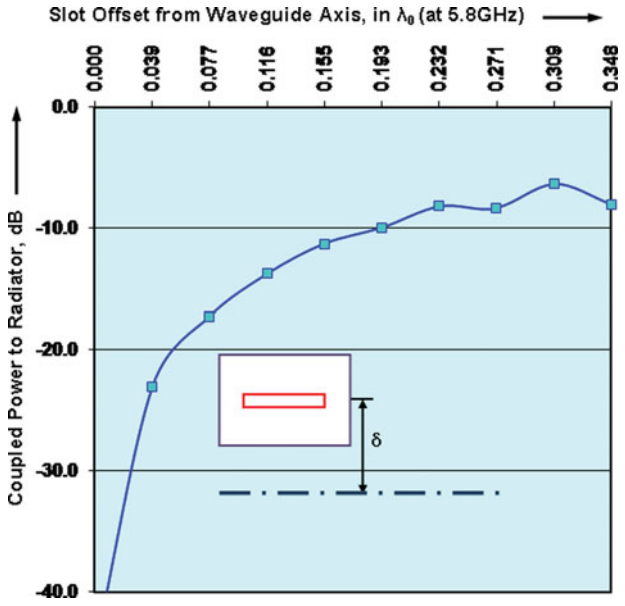

Fig. 2. Parametric variation of coupled power to prototype microstrip antenna with axial offset of coupling slot, δ mm.

The measurement vectors are derived for each principal plane for the given incident polarization. The measurement vector due to y-component of patch current for a φ-polarized wave in the $x = 0$ plane ($\theta = 90^\circ$), is

$$(P_1^{m1})^y_{\varphi x} = 2j \sin(k_0 d \sin\varphi) \frac{L_p(l\pi/W_p)}{-k_0^2\cos^2\varphi + (l\pi/W_p)^2} \times e^{jk_0 y_p \cos\varphi} \begin{pmatrix} 2 & \cos\left(k_0 \frac{w_p}{2}\cos\varphi\right);\ l\ odd \\ -2j & \sin\left(k_0 \frac{w_p}{2}\cos\varphi\right);\ l\ even \end{pmatrix}. \tag{6}$$

For l odd, the terms contribute a co-polarized pattern with a central peak whereas for l even, there is a boresight null resembling a cross-polarized pattern.

The measurement vector due to y-component of patch current for a y-polarized wave in the $y = 0$ plane ($\varphi = 90^\circ$):

$$(P_1^{m1})^y_{yy} = 8j \frac{e^{jk_0 x_p \cos\theta} \sin(k_0 d \sin\theta) \sin\left(k_0 \frac{L_p}{2}\cos\theta\right)}{k_0 \cos\theta (l\pi/W_p)};\ l\ odd$$
$$= 0;\ l\ even. \tag{7}$$

This function has a boresight peak for l odd but a null-field contribution for l even.

The slot makes minor contributions as it is chosen as non-resonant. The measurement vector due to x-component of

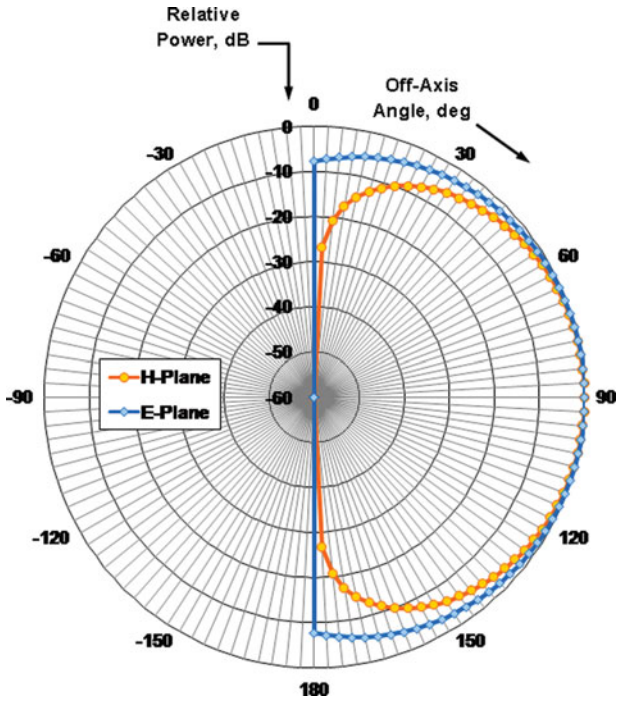

Fig. 3. MOM-computed principal plane radiation patterns for C-band prototype WGMPA element at 5.59 GHz.

https://doi.org/10.1017/S1759078713000548 Published online by Cambridge University Press

current for a y-polarized wave in $y = 0$ plane ($\varphi = 90^\circ$) is

$$(P_m^{m2})_{yy}^{x} = \frac{2\sin\theta W_s}{\eta}\frac{(m\pi/L_s)}{-k_0^2\cos^2\varphi + (m\pi/L_s)^2} \times 2\cos\left(k_0\frac{L_s}{2}\cos\varphi\right);\ m\ odd \quad (8)$$
$$-2j\sin\left(k_0\frac{L_s}{2}\cos\varphi\right);\ m\ even.$$

This function contributes co-polarized radiation for m odd or even but for the latter, there is a null in the plane of the slot.

Finally, the measurement vector for x-component of the current across the coupling slot for a φ-polarized wave in the $x = 0$ plane ($\theta = 90^\circ$) may be obtained as

$$(P_m^{m2})_{\varphi x}^{x} = \frac{8}{\eta}\frac{\sin\left(k_0\frac{W_s}{2}\cos\varphi\right)}{k_0\cos\varphi\left(m\pi/L_s\right)};\ m\ odd \quad (9)$$
$$= 0;\quad m\quad even.$$

For m odd, the terms contribute a cross-polar pattern with a boresight null and null-field for m even.

These expressions were used in (5) to obtain the net radiation pattern – Fig. 3 shows an example.

IV. OBTAINING LINEAR ARRAYS WITH WGMPA AS UNIT CELL AND ARRAY FACTOR FORMULATION

As alluded to above, linear arrays may conveniently be obtained by cascading WGMPA elements on the through-end of the feeding waveguide. Owing to the peculiar feeding medium, i.e. a continuous waveguide, the linear array becomes a series-fed structure with the intervening waveguide lengths deciding the inserted phase between the elements.

To obtain a broadside radiation pattern, all radiating elements of the resulting linear array need to be excited in-phase.

This can be forced equal to 360°; in which case the element spacing has to be λ_g, a choice that may lead to undue grating lobes. Fortunately, there is a more elegant solution. The coupling slots may be placed $\lambda_g/2$ apart resulting in out-of-phase excitation. However, by alternately placing the slots on either side of the waveguide longitudinal axis, the remaining 180° phase may be imparted resulting in broadside reinforcement without grating lobes (see Fig. 4).

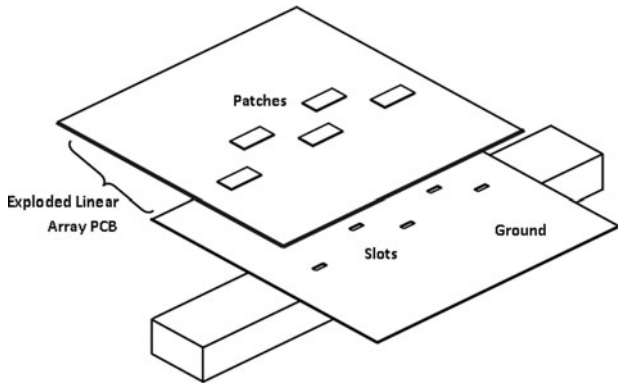

Fig. 4. Linear array of WGMPA's in staggered configuration.

This approach is followed for designing linear array modules using the C-band WGMPA prototype listed in the foregoing section. In accordance with the resonant frequency obtained for the prototype, the design of the arrays is also performed at 5.59 GHz. An inter-element spacing of $\lambda_g/2 =$ 35.91 mm was chosen. A nominal number of five radiating elements were selected to obtain a workable array length while providing enough freedom to tailor the pattern.

Since the individual radiating elements are staggered around either side of the waveguide median, the array is not strictly a linear array. Hence, for computing the array factor, the expression for arbitrary element positions is selected. This is well-documented in the literature [7] but is reproduced for completeness as below for a given far-field direction (θ, φ):

$$AF(\theta,\varphi) = \sum_{i=1}^{N}\frac{I_i}{I_0}e^{j\bar{k}(x_i\sin\theta\cos\varphi + y_i\sin\theta\sin\varphi + z_i\cos\theta)} \quad (10)$$

where (x_i, y_i, z_i) is the location of the ith array element and I_i is its excitation current compared to the minimum excitation I_0.

Design is carried out for two sample linear array cases.

V. FIVE-ELEMENT LINEAR ARRAY MODULES WITH UNIFORM AND DOLPH–CHEBYSHEV EXCITATIONS

To obtain a uniform amplitude taper across the array, a fixed transverse offset of ± 10 mm for the feeding slot was chosen on either side of the median line of waveguide. This choice is not critical since the elements are to be excited in equal amplitudes in this variant. However, $x_s = 10$ mm ensures a large fraction of power coupling through the feeding slots to the patches as indicated by the MOM results. This will yield high radiation efficiency and a good radiating structure from this design.

A uniformly-excited aperture is characterized by a relatively large first sidelobe level of ∼−13 dB. The sidelobe level may be reduced at the expense of boresight gain by applying a taper to the excitation amplitudes. With a tapered amplitude, the side elements contribute lesser to both the main beam as well as the side lobes resulting in lower levels of both. In terms of the Schelkunoff unit circle method [7], the relative power level in a direction is proportional to the product of the distances to all the roots. As a result, clustering the roots closer to $\psi = \pi$ will result in a reduction of the sidelobe levels in general. A procedure due to Dolph entails placing array factor roots at the appropriate position to obtain a symmetrical pattern and reduced side lobes exhibiting a behavior as per Chebyshev polynomials (see pp. 134 of [7]). This results in equalized side lobes at the specified relative level. An exact calculation gives the correct root positions for a 5-element case ± 88.82° and ± 145.16° for a −20 dB sidelobe level. This requires excitation of the elements in the following ratio:

1 : 1.60 : 1.93 : 1.60 : 1

https://doi.org/10.1017/S1759078713000548 Published online by Cambridge University Press

To obtain this distribution of amplitude excitations requires determination of the transverse offset of each coupling slot from the waveguide axes. The parametric behavior of the power coupling versus slot offset x_s presented in Fig. 2 is utilized to obtain the corresponding slot positions.

The offset for the central element that requires maximum power coupling is fixed at 10 mm as this is close to the maximum coupling level that may be achieved by the slot. The other two couplings are used to obtain the offsets for the end elements and the next inner elements respectively as:

6.64 mm and 8.71 mm.

These two cases are chosen as their expected outcome is well-known and as such may be considered as benchmarks. The MOM-based computations are carried out along the above lines. To further validate our findings, we have utilized an FEM-based commercial solver for the two cases (described next in Section VI). The results from both alternate simulation methods are presented in Section VII.

VI. FEM-BASED ANALYSIS OF LINEAR ARRAY MODULES

Ansoft® HFSS®, a commercial FEM-based e.m. solver, is used for simulation of both example linear array modules. For both cases, the ground plane size is truncated at a reasonable size beyond the radiating elements to allow all significant fringing fields to be included–determined through a few trials for convergence. Through similar considerations, the radiation enclosure required by HFSS®, the ABC is extended ~0.1λ either side beyond the substrate while the height is retained as ~0.8λ through a convergence check (see Fig. 5). Meshing operations to seed the substrate, patch, and slot are performed manually before execution and boundary conditions are defined appropriately.

The voltage standing wave ratio (VSWR) response is relatively broadband (see Fig. 6) for both cases. As the number of elements are few, through port match-termination provides a low-reflection response. A power coupling parameter, $P_{out} = 1 - |S_{11}|^2 - |S_{21}|^2$ is expected to yield a more sensitive means of detection of resonance. The plot of P_{out} (Fig. 7) indicates a distinct peak at 5.59 GHz. The results for the Dolph–Chebyshev case are similar and are not repeated.

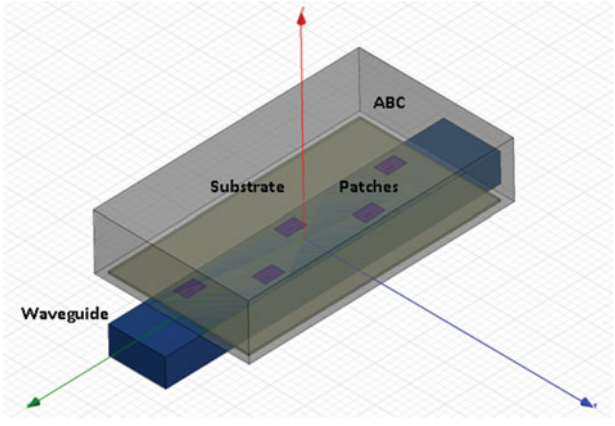

Fig. 5. Five-element linear array of waveguide shunt slot-fed microstrip antenna elements with uniform excitations.

The contour plots at the resonant frequency show an in-phase reinforcement of the fields radiating from the individual elements in the space toward the front of the substrate (see Fig. 8). The *E*-plane contours are close to that of a single element. The uniformly-excited case also shows similar plots.

VII. MOM-COMPUTED RADIATION PATTERN PLOTS AND COMPARISON TO FEM RESULTS

The computed radiation patterns for the linear array show behavior close to that expected for the 5-element uniformly-excited linear array configuration (see Figs 9 and 10).

The peak directivity is 11.509 dBi and half-power beamwidths in the principal planes are $16^\circ \times 72^\circ$. The *H*-plane pattern shows expected beam narrowing due to presence of five radiating elements. The two principal sidelobe levels are −14.43 and −18.18 dB, respectively. These are as expected; the minor difference being due to the element pattern roll-off from boresight. Furthermore element spacing corresponds to 0.67 λ_o; hence it differs from the standard case of $\lambda_o/2$.

FEM predicts field values in the rear half-plane where MOM does not on account of infinite ground assumption in Green's functions used. Pattern asymmetry, null-shift and null-filling as well as in-plane radiation are seen.

The *E*-plane patterns are shown since element staggering causes them to differ from those of a single element (Fig. 10). A slight beam asymmetry is also predicted by FEM compared to MOM.

For the case of Dolph–Chebyshev excitations, it is possible to visually discern the effect of the reduced excitation on the outer elements (compare Figs 9 and 11). The computed radiation patterns show expected sidelobe reduction due to tapered amplitude weights. The predicted peak directivity is 10.383 dBi which is about 1.1 dB lower than the uniformly-excited linear array module representing the penalty of sidelobe suppression. The half-power beamwidths in the principal planes are $18^\circ \times 86^\circ$ which also represents a main lobe enlargement versus the previous case. The two principal sidelobe levels are −18.62 and −19.38 dB, respectively. These are close to the intended equalized level of −20 dB. The differences are due to approximation in the excitation amplitudes actually realized by the given transverse offsets. It is possible to carry out a more accurate estimate of the offsets and a few design iterations to obtain a 20-dB suppression if desired. *E*-plane pattern predictions by the two analysis

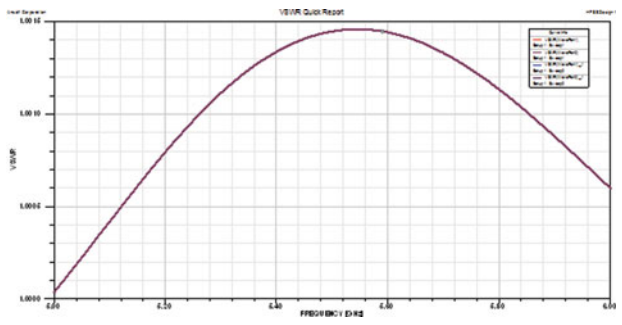

Fig. 6. Simulated VSWR for 5-element WGMPA linear array with uniform excitations.

https://doi.org/10.1017/S1759078713000548 Published online by Cambridge University Press

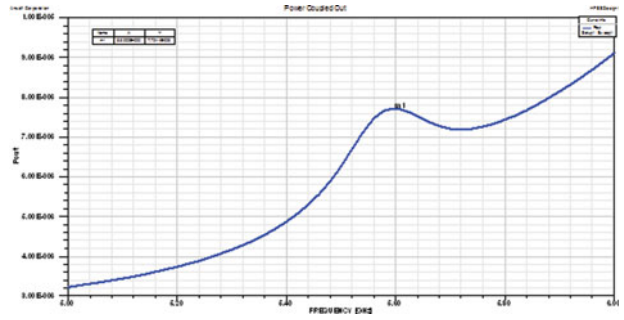

Fig. 7. Simulated coupled-power, P_{out} for 5-element WGMPA linear array with uniform excitations.

methods agree closely (Fig. 12). The predicted back lobe level is −21.89 dB which conforms to the uniform-excitation case.

Apart from a match of the far-field radiation patterns, for the sake of validation, the relative current (magnetic) strength across the slot predicted by MOM and HFSS® are compared. These are seen to match closely (see Fig. 13), the latter showing minor steps due to the discretization involved.

From the presented results, it is seen that the radiation pattern as well as slot current predictions using the developed MOM-analysis used together with array factor formulation for the two sample linear arrays closely match the results from the commercially-proven FEM-based e.m. simulator HFSS®. By implication, the MOM-based predictions may be said to be validated from the results presented. MOM provides a faster and computationally-efficient method for obtaining such arrays. Rigorous analysis with FEM may be carried out in the final stage to include finite-ground, mutual-coupling, and other effects. It is also evident that the proposed

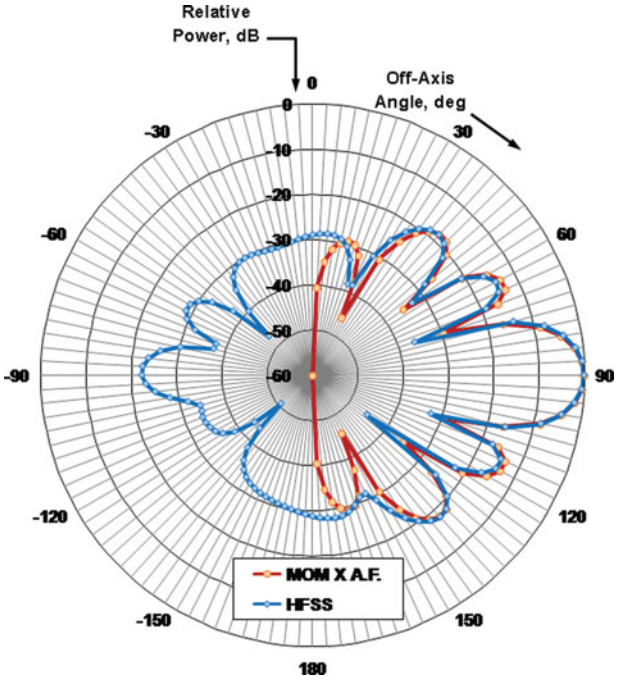

Fig. 9. Radiation patterns for uniformly-excited WGMPA linear array – MOM versus HFSS® simulations (*H*-plane).

WGMPA element provides a convenient means of varying the amplitude distribution along a series-fed linear array. The two sample distributions chosen for analysis suffice to illustrate the feasibility of choosing any tailored distribution which may then be quickly realized using the design data of Section III for a reduced, equalized sidelobe envelope here

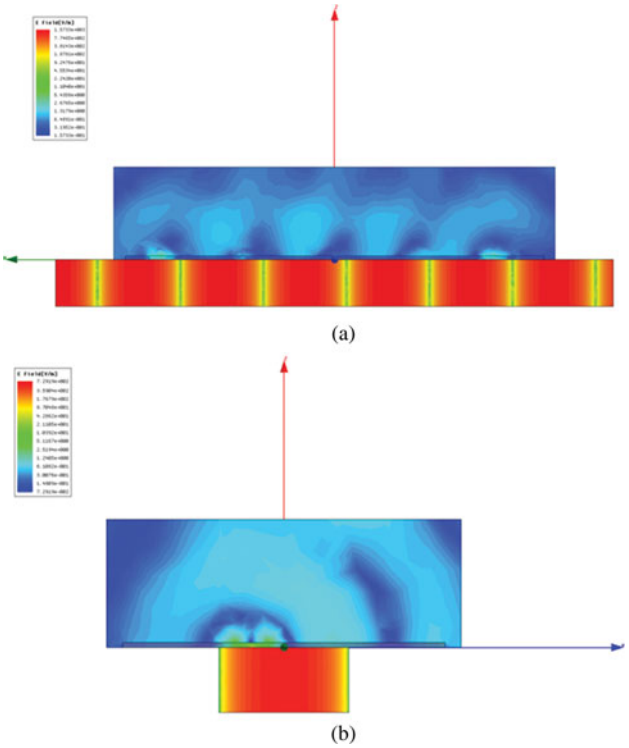

Fig. 8. HFSS®-computed E-field contours – for five-element linear array module Dolph-Chebyshev excitations – (a) *axial section* and (b) *cross section*.

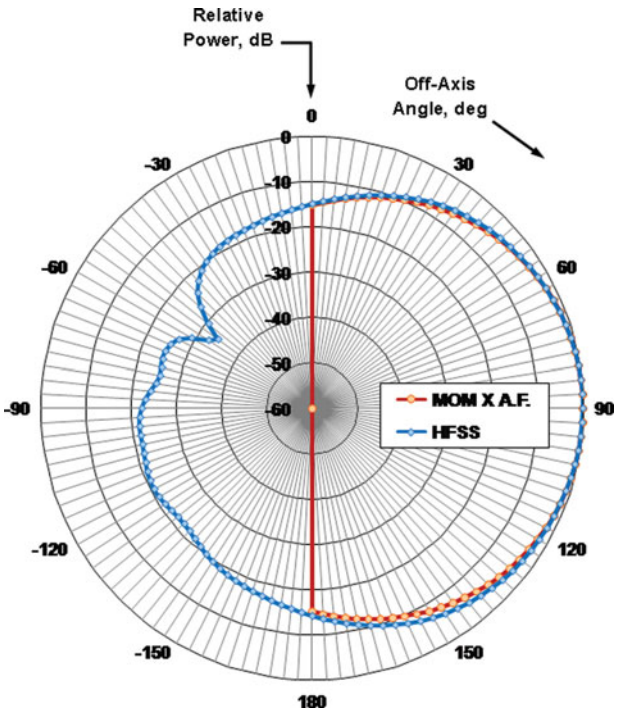

Fig. 10. Radiation patterns for uniformly-excited WGMPA linear array – MOM versus HFSS® simulations (*E*-plane).

https://doi.org/10.1017/S1759078713000548 Published online by Cambridge University Press

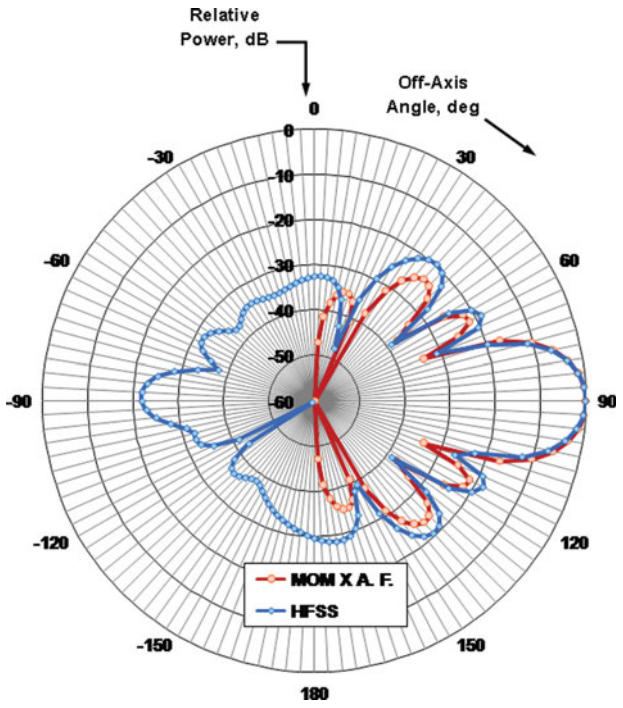

Fig. 11. Radiation patterns for Dolph-Chebyshev WGMPA linear array – MOM versus HFSS® simulations (*H*-plane).

and for other objectives in general. By extension, these 'stick' modules may be cascaded in the transverse direction although this has not been attempted presently. It may be mentioned here that due to the relatively large ground plane assumed at present, the aperture efficiency of the antenna may be small. This is primarily because the present variant is intended to demonstrate validation of the MOM analysis and to

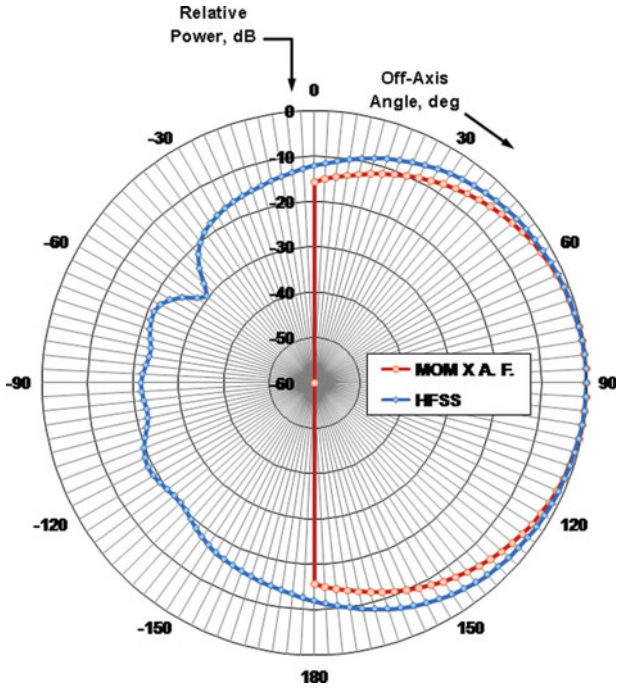

Fig. 12. Radiation patterns for Dolph-Chebyshev WGMPA linear array – MOM versus HFSS® simulations (*E*-plane).

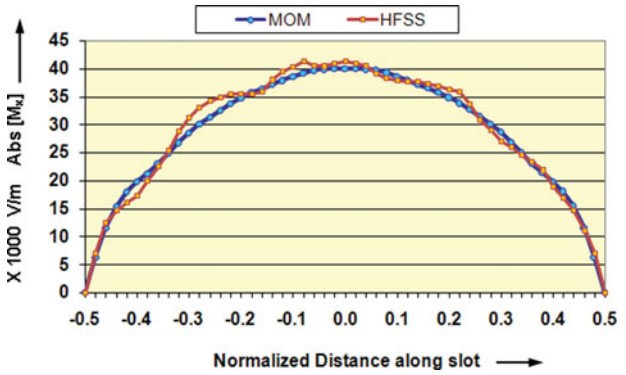

Fig. 13. Comparison of computed slot magnetic current for C-band antenna prototype: MoM versus HFSS.

illustrate the flexibility of varying amplitude distribution along the array axis. When the proposed linear array is stacked in the transverse direction to build a complete planar array, element packing efficiency will be higher and we can expect good aperture efficiency. However, this has not been attempted and the antenna design has not been optimized for the same at present.

VIII. CONCLUSION

This paper has presented some details of the MOM-analysis a WGMPA previously proposed by the authors, particularly the far-field terms for basis-functions on radiator geometry. The developed radiating element is used as a unit cell for building linear array modules (or sticks) by cascading a number of elements at the opposite waveguide end. As a proof-of-concept, a five-element linear array configuration has been selected and two types of excitations applied to it: uniform excitations and Dolph–Chebyshev tapered distribution for reduced side lobes. MOM-based pattern predictions for the WGMPA element have been used in conjunction with an array factor for arbitrarily-positioned elements to obtain the array patterns. Simulations show input characteristics as well as radiation patterns close to that expected. Both the configurations were also analyzed using an FEM-based simulation software. The results of this compare closely with the MOM predictions thus validating the developed analysis. The efficacy of WGMPA element is thus established for realizing linear array modules that, in turn, are amenable to obtaining full planar array configurations. Desired tailored distributions may be applied using the parametric studies presented herein as shown by the results of the Dolph–Chebyshev module presented in this paper.

ACKNOWLEDGEMENTS

The authors are grateful to Dr R. R. Navalgund, Director, SAC and Mr A. S. Kiran Kumar, Associate Director for their inspiring leadership and steadfast encouragement of truly technical pursuits. We are obliged to all our colleagues at SAC who spared time from their busy schedules to help us with suggestions and discussions. We appreciate warmly the help of Jigar Pandya, Alok Singhal, Jidesh, and Atrish Mukherjee regarding FEM analysis.

https://doi.org/10.1017/S1759078713000548 Published online by Cambridge University Press

REFERENCES

[1] Pozar, D.M.: An update on microstrip antenna theory and design including some novel feeding techniques. IEEE Antennas Propag. Soc. Newslett., **22**(5) (1986), 4–9.

[2] Kanda, M.; Chang, D.C.; Greenlee, D.H.: The characteristics of iris-fed millimeter-wave rectangular microstrip patch antennas, in IEEE AP-S Intl. Symp. Digest, May 1982.

[3] Ho, M.-H.; Hsu, C.-I.G.: Circular-waveguide-fed microstrip patch antennas. Electron. Lett., **41**(22) (2005), 1202–1203.

[4] Chang, W.; Schaubert, D.H.: Longitudinally polarized waveguide array using slot-patch element. Electron. Lett. **34**(13) (1998), 1326–1327.

[5] Wu, W.; Yin, J.; Yuan, N.: Design of an efficient X-band waveguide-fed microstrip patch array. IEEE Trans. Antennas Propag., **AP-55**(2007), 1933–1939.

[6] Sood, K.; Jyoti, R.; Sharma, S.B.: A waveguide shunt slot-fed microstrip patch antenna – analysis using the method-of-moments, manuscript submitted to IEEE Trans-AP (present status: editors' comments received, manuscript under revision).

[7] Elliott, R.S.: Antenna Theory and Design, Hoboken: IEEE Press Wiley-Interscience, NJ, 2003.

Dr. Khagindra Kumar Sood was born in Sangrur, Punjab, India in 1967. He received his B.E. in Electronics & Elect. Comm. Engineering from Thapar University, Patiala, Punjab, India in 1990. He received his M. E. in 1992 in Electronics & Communication Engineering from the Indian Institute of Technology (IIT Roorkee) (erstwhile University of Roorkee), Uttaranchal, India specializing in Microwave & Radar Engineering. His post-graduate work encompassed a waveguide shunt-slot feed for a microstrip patch antenna and the development of a method-of-moments code for the problem analysis. He completed his Ph. D. in 2013 in Antenna & Microwave Engineering from Nirma University, Ahmedabad, Gujarat, India working on "Planar Broadband Microstrip Radiators in Conjunction with Optimum Feeding Techniques". Since 1992 he has been with the Antenna Systems Group at the Space Applications Centre (SAC) of the Indian Space Research Organization (ISRO) at Ahmedabad, Gujarat, India. Mr. Sood has also been a Guest Scientist at the German Aerospace Centre (DLR) at Oberpfaffenhofen, Bavaria, Germany over the period 1999-2000 where he worked on technologies for active terminal antennas at K_a- and V-bands.

At ISRO, he has been involved with the design and development of antennas, feed systems and associated passive components for spaceborne as well as ground-based applications. His key areas of interest are shaped reflectors, dual-gridded reflectors, multiple-beam antennas, unfurlable antennas, large Cassegrain earth-station antennas and feed horns, OMT's, etc. for these antennas. He has been Deputy Project Director, Communication Payload Antennas for important ISRO communication satellite projects. In this capacity, some of his notable contributions are segmented shaped reflector for enhanced inter-beam isolation for GSAT-4, unfurlable antenna for INSAT-4E and indigenous dual-gridded reflectors for INSAT-4G/GSAT-8. He has published some of his work in Electronics Letters, co-authored several technical papers and is an inventor/co-inventor in eight patent applications relating to antennas with high beam isolation, low cross-polarization and multimode tracking antennas. He is currently the Division Head of the Satellite Communication Antennas Division within the Antenna Systems Group at SAC. He is responsible for the design and development of antenna systems related to satellite communications, satellite-based navigation and satellite ground terminal antennas for various applications.

Rajeev Jyoti received his Master of Science in Physics and M. Tech. in Microwave Electronics from Delhi University, Delhi, India in 1984 and 1986 respectively. Since 1987, he is involved in the development of antennas for satellite communication at Space Applications Centre (SAC), Indian Space Research Organization (ISRO), Ahmedabad, India. Presently, he is Group Director of Antenna Systems Group at SAC, ISRO, India. He has more than 25 years experience in development of space borne and ground antennas at SAC. He has contributed significantly in design, analysis and development of microwave antennas namely gridded antenna, multiple beam antennas and phased array antennas for INSAT/GSAT, RISAT, DMSAR projects.

Mr. Rajeev Jyoti is Fellow Member of IETE India, Senior Member of IEEE, USA, and Chair of Joint Chapter of IEEE AP and MTT, Ahmedabad. He has published more than 55 papers in various conferences and referred journals. He has 14 patents to his credit. He was awarded UN ESA Long term fellowship in Antenna & Propagation at ESTEC/ESA Noordwijk, Netherland.

Shashi Bhushan Sharma was born in Moradabad, India in 1947. He received B.E. in Electronics and Communication, M.E. in Microwave Engineering, both from the University of Roorkee in 1970 and 1972 respectively and Ph.D. degree in Microwave Engineering in 1987 from Gujarat University. He has more than 32 years of academic and diversified research and development experience in the design and development of antenna systems for satellite communication and remote sensing. He has about 110 publications to his credit. He was honored in 1992 with Dr. Vikram Sarabhai Research Award and Astronautical Society of India Award, 2003 for his outstanding contributions to the development of various types of antenna systems for ground, airborne, and spaceborne systems. He is presently Deputy Director, Antenna Systems Area (ASA), Space Application Center, ISRO, India.

https://doi.org/10.1017/S1759078713000548 Published online by Cambridge University Press